

Supplementary Information for:

Harnessing the central dogma for stringent multi-level control of gene expression

F. Veronica Greco, Claire S. Grierson and Thomas E. Gorochowski

Supplementary Notes	Page
Supplementary Note 1: Derivation of mathematical models	2
Supplementary Note 2: MLC toolkit user guide	3
Supplementary Figures	
Supplementary Figure 1: Growth curves	5
Supplementary Figure 2: STAR ₂ performance comparison	6
Supplementary Figure 3: Plasmid maps for the MLC toolkit	7
Supplementary Figure 4: Plasmid maps for the gene expression controllers used	8
Supplementary Tables	
Supplementary Table 1: Model parameters	9
Supplementary Table 2: Genetic parts used in this study	10
Supplementary References	12

Supplementary Note 1: Derivation of mathematical models

To explore how single- and multi-level regulation affected the output protein production rate as a function of an input inducer chemical concentration, we derived mathematical models for each type of system. For the single-level controller we defined equations to track the concentration of GOI transcripts R and protein P as:

$$\frac{dR}{dt} = \alpha_I - \gamma_R R, \quad (1)$$

$$\frac{dP}{dt} = \alpha_P R - \gamma_P P. \quad (2)$$

Here, α_I is the production rate of GOI transcripts, α_P is the production rate proteins per transcript, and γ_R and γ_P are first-order degradation rates of the transcripts and output proteins, respectively. In this system, α_I is directly related to the activity of the P_{L1} promoter (**Figure 1C**). To capture a realistic response of a promoter for a small molecule sensor (e.g. the P_{tac} system) that we might use as input to the controller, we made use of empirically measured steady-state response functions that fit to a Hill equation such that

$$\alpha_I = f(x) = y_{\min} + (y_{\max} - y_{\min}) \frac{x^n}{K^n + x^n}. \quad (3)$$

Here, x is the concentration of the inducer (e.g. small molecule), y_{\min} and y_{\max} are the minimum and maximum activities of the P_{L1} promoter, K is the inducer concentration where the P_{L1} promoter activity is half its maximum, and n is the cooperativity.

For the MLC, we extended this model to include additional states for the concentrations of the $L2$ regulator S , and the complex C of the GOI transcript with the $L2$ regulator that forms through non-cooperative RNA-RNA hybridisation. By assuming that only these complexes can be translated into output protein, we end up with the following set of equations:

$$\frac{dR}{dt} = \alpha_I - k_{C+}RS + k_{C-}C - \gamma_R R, \quad (4)$$

$$\frac{dS}{dt} = \alpha_S - k_{C+}RS + k_{C-}C - \gamma_S S, \quad (5)$$

$$\frac{dC}{dt} = k_{C+}RS - k_{C-}C - \gamma_C C, \quad (6)$$

$$\frac{dP}{dt} = \alpha_P C - \gamma_P P, \quad (7)$$

where k_{C+} and k_{C-} are the binding and unbinding rates of the GOI transcript with the $L2$ RNA-based regulator.

To analyse the behaviour of these systems, numerical simulation of these ODEs was performed using the `odeint` function of the `SciPy.integrate` Python package and biologically realistic parameters assuming the input sensor behaved similarly to the P_{tac} system (**Supplementary Table 1**).

Supplementary Note 2: MLC toolkit user guide

The MLC toolkit is composed of a set of plasmids and assembly rules to create controllers in a combinatorial manner. It includes a backbone plasmid called pMLC-BB1 that is used to hold newly build controllers and a set of 8 types of part plasmid (pA–pH) corresponding to the individual blocks that make up a controller (**Figure 2A**). pMLC-BB1 is based on the pET28a(+) plasmid and contains a pBR322 origin of replication, kanamycin resistance marker and expression cassette for an orange fluorescent protein (*ofp*) gene that is highly visible in transformed cells. The *ofp* expression cassette is flanked by *Bsa*I sites such that it is removed before insertion of a fully assembled MLC. To minimise controller malfunctions due to individual part failure, the orientation of each transcriptional unit has been chosen such that potential transcriptional read-through at any terminator does not cause unwanted expression of other controller elements. The toolkit has also been designed to ensure the accurate and rapid assembly of new designs by minimising the chance of incorrect assembly through the selection of 4 bp overhangs with low cross reactivity and the use of a fluorescent protein drop out upon successful insertion of a controller construct into the backbone to reduce the subsequent screening/sequencing of transformants needed to verify a perfect assembly.

Creating new parts

Parts for each block of a controller can be created in the form of pre-cloned plasmids, amplicons or even annealed complementary oligos if the length is short. Pre-cloned plasmids are the preferred method as this reduces the chance of part mutations. Amplicons are easy to generate by PCR and allow for the easy addition of 5' and 3' sequences needed for assembly, however, also tend to see higher numbers of mutations. Complementary oligos annealed to create a double stranded DNA part are ideal for smaller sequences up to 60 nt, although again using this method will lead to the highest error rates in the final parts produced. Every new part must be flanked by a standardised sequence that is used to create the necessary single stranded overhangs that are used for correct assembly. These sequences contain a *Bsa*I restriction site and a specific 4 bp overhang. The following table provides details of the necessary 5' and 3' sequences that are needed.

Part block	Sequence to add at 5' end	Sequence to add at 3' end
A	NNNNNNGGTCTCAgtga	ggagTGAGACCNNNNNNN
B	NNNNNNGGTCTCaggag	aggtTGAGACCNNNNNNN
C	NNNNNNGGTCTCAaggt	gcttTGAGACCNNNNNNN
D	NNNNNNGGTCTCagctt	cgctTGAGACCNNNNNNN
E	NNNNNNGGTCTCacgct	ccgcCGAGACCNNNNNNN
F	NNNNNNGGTCTCaccgc	catcCGAGACCNNNNNNN

G	NNNNNNGGTCTC <u>catc</u>	tact TGAGACCNNNNNN
H	NNNNNNGGTCTC <u>tact</u>	tgcc TGAGACCNNNNNN

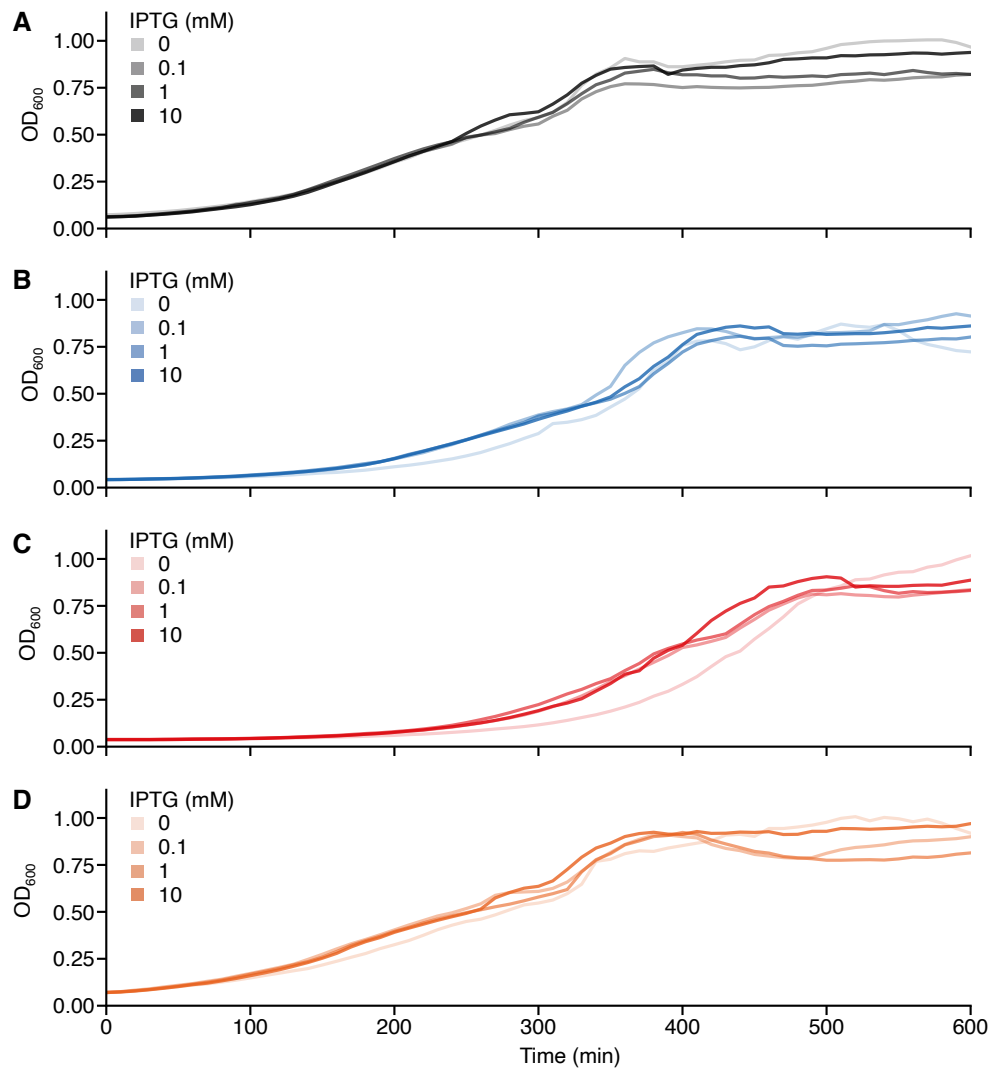
Underlined sequences denote BsaI recognition sites used for Golden Gate assembly. Bold lowercase sequences denote 4 bp overhangs generated after digestion by BsaI which are used for assembly. The six undefined bases at the 5' and 3' ends are optional but help improve digestion efficiency.

Assembling new controllers

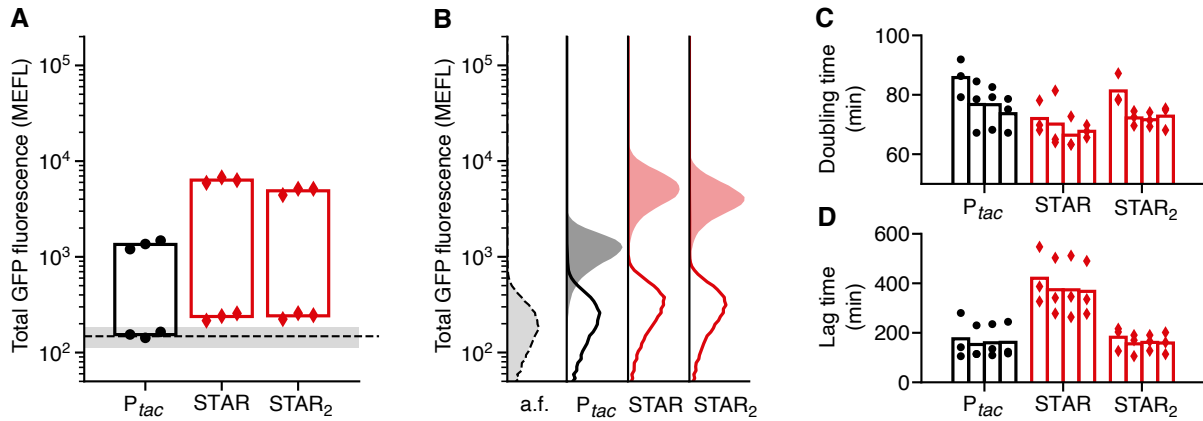
Assembly of a controller is performed using a standard Golden Gate reaction. We recommend the use of the NEB Golden Gate Assembly Kit (BsaI-HFv2, E1601) and have found that assemblies can be scaled down using this kit to a quarter of their normal volume (5 μ L) with still large numbers of successful transformants produced for chemically competent *E. coli* DH10- β cells using 2 μ l of the reaction mix. Each reaction should include the backbone plasmid and a single plasmid type for each of the blocks in the controller (**Figure 2A**). Although we rarely see mutations in the part sequences, there is a tendency for mutations to occur within the 4 bp overhangs used for assembly. Therefore, it is recommended that all controllers are fully sequence verified before use.

Assembling single-level controllers using the MLC toolkit

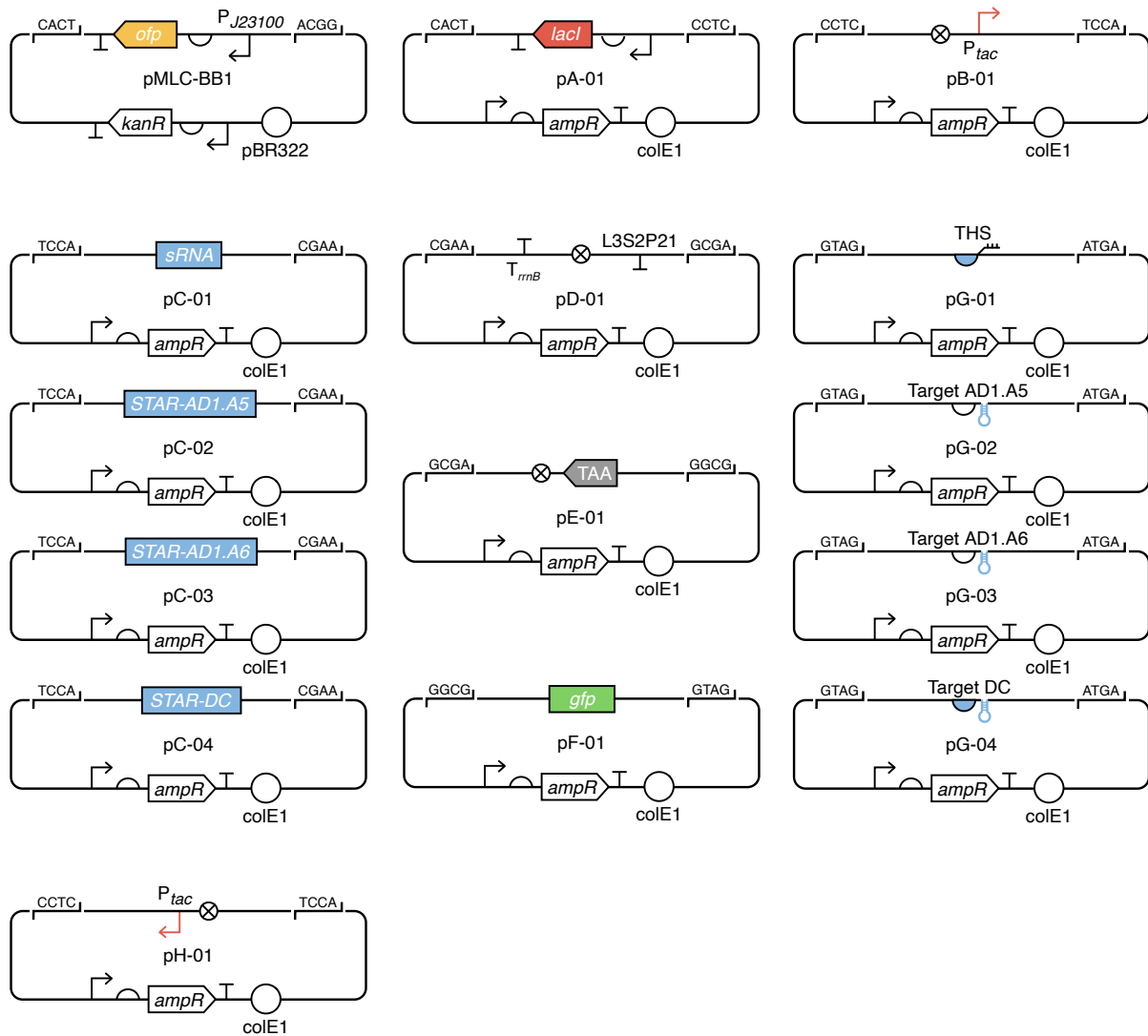
Although the toolkit is tailored to produce MLCs, it is possible to create SLCs by substituting several blocks with a specially designed spacer. Specifically, blocks B and C can be replaced by a single spacer element ('BC-spacer', **Supplementary Table 2**) that is able to assemble with block A at its 5'-end and block D at its 3'-end. As mutations in this part are less problematic, we have used annealed oligos to produce this part for creating the P_{tac} SLC. In addition, the removal of the L2 regulator also requires the use of a standard RBS part for block G. We include a strong RBS part in the toolkit for this use ('RBS', **Supplementary Table 2**).



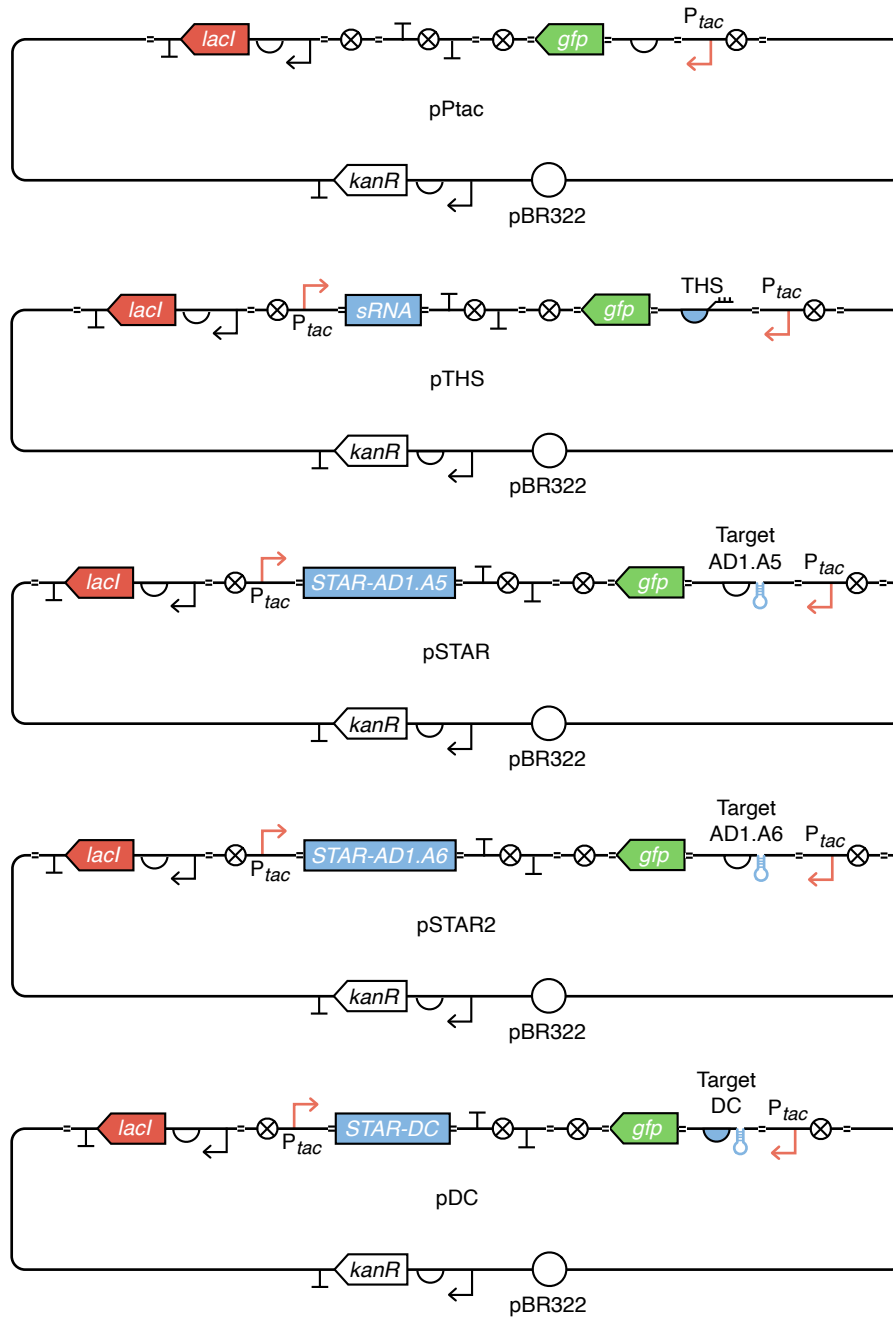
Supplementary Figure 1: Growth curves. Time course measurements of the optical density at 600nm (OD₆₀₀) of *E. coli* DH10-β cells harboring (A) pPtac, (B) pTHS, (C) pSTAR and (D) pDC plasmids in the presence of different concentrations of IPTG.



Supplementary Figure 1: $STAR_2$ performance comparison. Data for the P_{tac} and STAR designs shown for comparison. **(A)** Total GFP fluorescence for ‘off’ and ‘on’ input states (0 and 1 mM IPTG, respectively). Points show the three biological replicates for each controller and condition (black circles, P_{tac} ; red diamonds, STAR, $STAR_2$). Black dashed line denotes the mean fluorescence of cell autofluorescence (a.f.) controls containing no plasmid with grey shared region showing ± 1 standard deviation of 11 biological replicates. Fluorescence given in calibrated molecules of equivalent fluorescein (MEFL) units. **(B)** Flow cytometry distributions of total GFP fluorescence for ‘off’ (line) and ‘on’ (shaded) input states. Cell autofluorescence (a.f.) controls containing no controller are shown by black dashed line and light grey filled distributions. **(C)** Doubling time of cells harbouring single- and multi-level controllers for varying concentrations of IPTG (bars left to right for each design: 0, 0.1, 1, 10 mM IPTG). **(D)** Lag time calculated as the time to reach an $OD_{600} = 0.15$ after inoculation of cells harbouring controllers for varying concentrations of IPTG (bars left to right for each design: 0, 0.1, 1, 10 mM IPTG).



Supplementary Figure 3: Plasmid maps for the MLC toolkit. Genetic diagrams are shown using SBOL Visual symbols. Bsal restriction sites flanking each part are shown with their 4 bp overhang sequence after digestion that is used for assembly. The *gfp* part in plasmid pF-01 is in a reverse orientation and lacks a stop codon. The *gfp* open reading frame is completed after assembly with plasmid pE-01 which includes a TAA stop codon.



Supplementary Figure 4: Plasmid maps for the gene expression controllers used. Genetic diagrams are shown using SBOL Visual symbols and include the scars introduced between core elements of the genetic template.

Supplementary Table 1: Model parameters

Parameter	Description	Value(s)	Units	Refs.
α_I	Transcription rate of input promoter	0.04–100	transcript min ⁻¹	[1,2]
α_P	Translation rate of sRNA:transcript complex	5	protein complex ⁻¹ min ⁻¹	[3]
k_{C+}	sRNA:transcript complex association rate	0.0257	complex transcript ⁻¹ min ⁻¹	[4]
k_{C-}	sRNA:transcript complex disassociation rate	0.0067	transcript complex ⁻¹ min ⁻¹	[4]
γ_R	Transcript degradation rate	0.231	min ⁻¹	[5]
γ_S	sRNA degradation rate	0.231	min ⁻¹	[5]
γ_C	sRNA:transcript complex degradation rate	0.231	min ⁻¹	[5]
γ_P	Output protein degradation rate	0.035	min ⁻¹	[6]
y_{\min}	Minimum input promoter activity	0.04	transcript min ⁻¹	[1,2]
y_{\max}	Maximum input promoter activity	100	transcript min ⁻¹	[1,2]
K	Concentration of input inducer at which sensor output is half-maximal	134	mM	[1]
n	Cooperativity of input sensor system	1.9	–	[1]

Supplementary Table 2: Genetic parts used in this study.

Plasmid	Part	Sequence ^a	Ref.
pA1	<i>lacI</i> -TU	<u>GGTCTCAgtga</u> AGTGAAGAAAAGAAAAAGGCCGAGAGCGGCCTTTTTAGTTAGATCGGAC CCCACATCTCACTGCCCGCTTCCAGTCGGGAAACCTGTCGTGCCAGTGCATTAATGA ATCGGCCAACCGCGCGGGGAGAGGCGGTTTGCCTATTGGGCGCCAGGGTGGTTTTCTTT TCACCAGTGAGACTGGCAACAGCTGATTGCCCTCACCGCCTGGCCCTGAGAGAGTTGC AGCAAGCGGTCCACGCTGGTTTGGCCAGCAGGCGAAAAATCCTGTTTATGGTGGTTAA CGGCGGGATATAACATGAGCTATCTTCGGTATCGTCGTATCCCACTACCGAGATATCCG CACCAACGCGCAGCCCGGACTCGGTAATGGCGCGCATTGCGCCAGCGCCATCTGATCG TTGGCAACCAGCATCGCAGTGGGAACGATGCCCTCATTAGCATTGTCATGGTTTGTG AAAACCGGACATGGCACTCCAGTCGCCCTCCCGTTCCGCTATCGGCTGAATTTGATTGC GAGTGAGATATTTATGCCAGCCAGCCAGACGCGAGACGCGCCGAGACAGAACTTAATGGG CCCGCTAACAGCGCATTTGCTGGTGACCCAATGCGACCAGATGCTCCACGCCAGTCCG CGTACCGTCCCTCATGGGAGTAAATAACTGTTGATGGGTGTCTGGTCAGAGACATCAA GAAATAACGCCCGGAACATTAGTGCAGGCAGCTTCCACAGCAATGGCATCCTGGTCATCC AGCGGATAGTTAATGATCAGCCCACTGACGCGTTGCGCGAGAAGATTGTCACCGCCGC TTTACAGGCTTCGACGCGCTTCGTTCTACCATCGACACCACCAGCTGGCACCCAGTT GATCGGCGGAGATTTAATCGCGCGACAATTTGCGACGGCGGTGACAGGCCAGACTG GAGGTGGCAACGCCAATCAGCAACGACTGTTTCCCGCCAGTTGTTGTGCCACGCGGTT GGGAATGTAATTCAGCTCCACCATCGCCGCTTCCACTTTTCCCGCGTTTTCGAGAAA CGTGGCTGGCTGGTTACCACGCGGAAACGGTCATATAAGAGACACCGCCATACCT GCGACATCGTATAACGTTACTGGTTTCATATTACCTCCATGAATGGATCTCTCCGG GCGCTATCATGCCATACCGCAAAGGTTTTTACCATTGATGGCGCGCCGCGCTGGG AATCTGAGACATGAGTCAAGATATTTGCTCGGTAACGTATGCTggagTGAGACC	[7]
pB1	<i>P_{tac}</i>	<u>GGTCTCAaggag</u> TGTTGACAATTAATCATCGGCTCGTATAATGTGTGGAATTTGTGAGCGC TCACAATTagggtTGAGACC	[7]
pC1	STAR- pT1810-DC	<u>GGTCTCAagggt</u> AACAAAAATAAGCAATAAGGAATCGCTCACCCAAAGGATCTgcttTGA GACC	[8]
pC2	STAR- AD1.A5	<u>GGTCTCAagggt</u> TGAAGTGTATACATTTCCCGCTGCTCCAACATTTATACAACATAATTA AACAATTCAGTGTAAAACTgcttTGAGACC	[9]
pC3	STAR- AD1.A6	<u>GGTCTCAagggt</u> TGAAGTGTATACATTTCCCGCTGCTCCAACATTTATACAACATAATTA AACAATTCAGTGTAAAACTTTCTTAGACgcttTGAGACC	[9]
pC4	sRNA-THS	<u>GGTCTCAagggt</u> GGGACATATTGGACCCGTTTCCAATAGGTGAACAAGACGATAGAACAA GCATTTGCACTTATAGAgcttTGAGACC	[10]
pD1	TrrnB- L3S2P21	<u>GGTCTCAgctt</u> ATAAAACGAAAGGCTCAGTCGAAAGACTGGGCCTTTTCGTTTTATCTGT TGTTTGTGCGGTGAACGCTCTCTGAGTAGGACAAAATCCCGGGAGCGGATTTGAACGT TGCGAAGCAACGGCCCGGAGGTTGGCGGCAGGACGCCGCCATAAATGCCAGGCATC AAATTAAGCAGAAGGCCATCCTGACGGATGGCCTTTTGGCCCCGACCCTTAGACTCTG TACTCAGGACAAAACGAAAAAGGCCCCCTTTCCGGAGGCTCTTTTCTGGAATTT GGTACCGAGcgtTGAGACC	[11]
pE1	Spacer-TAA	<u>GGTCTCAcgtt</u> AGTTGTATCGTACGTCGGTCTAGGAATCGTTTAGccgcCGAGACC	—
pF1	<i>gfp</i>	<u>GGTCTCAccgc</u> CTCACTTATACAACATCCATGCCTAAAGTAATCCCGCCGCGGTTA CGAACTCCAAAAGGACCATGTGATCAGCTTTCATTTGGGTCTTCGATAATTTGGAT TGTGTACTCAGGTAGTGATTGTCAGGAAGTAAACCGGGCCGTCGCCAATGGGTGTGTT TTGTTGATAATGGTCAGCAATTCACGCTGCCATCCTCAATGTTGTGACGAATCTTGA AATTTACCTTAATCCCGTTCTTCTGCTTGTGAGCATGATATACAGTTGTGCGAATTA TAGTTACTCCAGTTTATGTCCAAAATGTTGCCATCTCTTTAAAGTCAATGCCTTT CAATTCATGCGATTCACTAACGTATCCCCCTCAAACCTGACCTCGGCGCGTGTCTTAT AGTTCCCGTCATCCTTGAAGAAGATTGTGCGCTTTCACATAGCCTTCTGGCATTGCA GATTTAAGAAGTCGTGCTGCTTCATGTGATCTGGTAACCGGAGAAACATTGGACCCC GTATGTAAGTGTGTAACCAGAGTTGGCCAGGGGACTGGAAGTTTTCTGTAGTACAAA TGAACCTAAGCGTCAATTTGCCGTAAGTAGCGTCGCCCTTCGCCCTCGCCGCTAACCGAA AACTTATGACCATTAACGTCCCCATCCAACCTCAACCAAGATGGGTACAACGCCTGAAA CAGCTCCTCTCCTTACTcactTGAGACC	—
pG1	Target- pT181- DC+RBS	<u>GGTCTCAcactc</u> AAAAAATCGACTCCTTAATCTCAATTTTCGTTTAAAGGAATCGCTCACCC AactTGAGACC	[8]
pG2	Target- AD1.S5+RBS	<u>GGTCTCAcactc</u> AGATCCTTCCCTCCTAGATCCAAAAAAGCGGGGAATATATACATGA ACTGTATACATTTCCCGCTGCTCCAACATTTATACAACATAATTAACAACATTCAGTGA AAAACTactTGAGACC	[9]

pG3	Target-AD1.S6+RBS	<u>GGTCTC</u> catc AGATCCTTCCTCCTAGATCCAAAAAAAAAGCGGGGAATATATACATGA ACTGTATACATTCCCCGCTGCTCCAACATTTATACAACATAATTAACAATTCACTGTGTA AAAACTTTTCCTAGACT tact <u>TGAGACC</u>	[9]
pG4	Target-THS	<u>GGTCTC</u> catc ACGCTTGTTCATGTCTTGTCTCCTCTGTTTCAAGACGATAGAACAA GCATTTGCACTTAT tact TGAGACC	[10]
pH1	P _{tac}	<u>GGTCTC</u> tact AATTGTGAGCGCTCACAAATCCACACATTATACGAGCCGATGATTAAT TGTCAACA tgcc TGAGACC	[7]
_ _b	RBS	Fwd: catc AGATCCTTCCTCCTAGATCCGCATCCGGGC Rev: agta GCCCCGGATGCGGATCTAGGAGGAAGGATCT	–
_ _b	BC-spacer ^c	Fwd: ggag CTCGTTTCATCCCGTGGGACATCAAGCTTCGCCTTGATAAA Rev: aagc TTTATCAAGGCGAAGCTTGATGTCCCACGGGATGAACGAG	–

- Underlined sequences denote Bsal recognition sites used for Golden Gate assembly. Bold lowercase sequences denote 4 bp overhangs generated after digestion by Bsal which are used for assembly.
- No plasmid was used for these parts. Instead, due to their short length complementary oligos were annealed (**Methods**) to generate double-stranded DNA parts with necessary single-stranded overhangs for assembly.
- This spacer is used to replace block B and C in an assembly when no L2 regulation is present.

Supplementary References

- [1] Stanton B.C., Nielsen A.A.K., Tamsir A., Clancy K., Peterson T. & Voigt C.A. (2014) Genomic mining of prokaryotic repressors for orthogonal logic gates. *Nature Chemical Biology* **10**, 99–105.
- [2] Kennell D. & Riezman H. (1977) Transcription and translation initiation frequencies of the *Escherichia coli lac* operon. *Journal of Molecular Biology* **114**, 1–21.
- [3] Pai A. & You L. (2009) Optimal tuning of bacterial sensing potential. *Molecular Systems Biology* **5**, 286.
- [4] Xu S., Zhan J., Man, B., Jiang, S. Yue W., Gao S., Guo C., Liu H., Li Z., Wang J. & Zhou Y. (2017) Real-time reliable determination of binding kinetics of DNA hybridization using a multi-channel graphene biosensor. *Nature Communications* **8**, 14902.
- [5] Bernstein J.A., Khodursky A.B., Lin P.-H., Lin-Chao S. & Cohen S.N. (2002) Global analysis of mRNA decay and abundance in *Escherichia coli* at single-gene resolution using two-color fluorescent DNA microarrays. *Proceedings of the National Academy of Sciences USA* **99**, 9697–9702.
- [6] Liang S.-T., Ehrenberg M., Dennis P. & Bremer H. (1999) Decay of *rplN* and *lacZ* mRNA in *Escherichia coli*. *Journal of Molecular Biology* **288**, 521–538.
- [7] Meyer A.J., Segall-Shapiro T.H., Glassey E., Zhang J. & Voigt C.A. (2019) *Escherichia coli* “Marionette” strains with 12 highly optimized small-molecule sensors. *Nature Chemical Biology* **15**, 196–204.
- [8] Westbrook, A.M. & Lucks, J.B. (2017) Achieving large dynamic range control of gene expression with a compact RNA transcription–translation regulator. *Nucleic Acids Research* **45**, 5614–5624.
- [9] Chappell, J., Takahashi, M.K., Lucks, J.B. (2015) Creating small transcription activating RNAs. *Nature Chemical Biology* **11**, 214–220.
- [10] Green, A.A., Kim, J., Ma, D., Silver, P.A., Collins, J.J. & Yin, P. (2017) Complex cellular logic computation using ribocomputing devices. *Nature* **548**, 117–121.
- [11] Chen Y.-J., Liu P., Nielsen A.A.K., Brophy J.A.N., Clancy K., Peterson T. & Voigt C.A. (2013) Characterization of 582 natural and synthetic terminators and quantification of their design constraints. *Nature Methods* **10**, 659–664.